PROCEEDINGS OF SCIENCE

Low-x physics at LHCb

Lucas Meyer Garcia[a,*] **on behalf of the LHCb Collaboration**

[a] *University of Maryland, College Park, MD 20742 USA*

E-mail: lucas.meyer.garcia@cern.ch

The LHCb detector, with its unique forward geometry, provides unprecedented kinematic coverage at low Bjorken-x values, down to 10^{-6}. LHCb 's excellent momentum resolution, vertex reconstruction and particle identification allow precision measurements down to very low hadron transverse momentum. In this report, recent studies of exclusive vector boson production in proton-proton and heavy ion collisions will be presented. These studies include the central exclusive production (CEP) of charmonium vector mesons in pp collisions, as well as their production in ultra-peripheral Lead-Lead collisions (UPC). Additionally, the production of exotic meson candidates in diffractive proton-proton collisions, previously observed only in $B^+ \to J/\psi \phi K^+$ decays, is reported. Future prospects for further investigations into low-x phenomena with the LHCb detector in Run 3 are also explored.

The European Physical Society Conference on High Energy Physics (EPS-HEP2025)
7-11 July 2025
Marseille, France

*Speaker

PoS(EPS-HEP2025)228

1. Introduction

Central exclusive production (CEP) in proton-proton collisions is a diffractive process where the protons interact elastically through the exchange of a colorless object (photons or Pomerons). Ultra-peripheral heavy-ion collisions (UPC) are diffractive processes also mediated by photons or Pomerons where the nuclei collide with impact parameter greater than the sum of their radii, suppressing short-range interactions and favoring electromagnetic processes [1]. Both processes are characterized by the presence of large rapidity gaps, since the incoming particles are only marginally deflected and escape detection. Consequently, only the centrally produced system is detected, providing a clean experimental signature. At LHCb, measurements of CEP can help constrain the proton gluon PDF at Bjorken-x values down to 10^{-6}, while measurements of UPC may provide constraints for the nuclear gluon PDF down to 10^{-5}. These measurements may also help elucidate the nature of the Pomeron, while UPC's provide an excellent laboratory to study nuclear shadowing effects at low-x. The LHCb collaboration has measured exclusive processes in pp and PbPb collisions at different centre-of-mass energies [2–13]. In this report, the diffractive production of vector mesons in pp [9, 12] and PbPb [8, 10, 13] collisions, based on data collected at LHCb during Run 2 of LHC, is presented.

2. The LHCb experiment

The LHCb detector [14, 15] is a single-arm forward spectrometer designed for the study of particles containing b or c quarks. The detector employs a high-precision tracking system which includes a silicon-strip vertex detector (VELO) surrounding the interaction region. Different types of charged hadrons are distinguished using information from two ring-imaging Cherenkov detectors. Photons are identified by a calorimeter system consisting of scintillating-pad (SPD) and preshower detectors, an electromagnetic and a hadronic calorimeter. Muons are identified by a system composed of alternating layers of iron and multiwire proportional chambers. The LHCb provides full coverage in the pseudorapidity range $2 < \eta < 5$, with additional coverage by VELO at $-3.5 < \eta < -1.5$ and $1.5 < \eta < 5$. This is further extended by the HeRSCheL detector [16], a system of forward shower counters consisting of scintillating planes, to $-10 < \eta < -5$ and $5 < \eta < 10$. The online event selection is performed by a trigger, which consists of a hardware stage, based on information from the calorimeter and muon systems, followed by a software stage, which applies a full event reconstruction.

3. Measurement of exclusive J/ψ and $\psi(2S)$ production at $\sqrt{s} = 13$ TeV

The CEP of J/ψ and $\psi(2S)$ is studied [12] using data from proton-proton collisions corresponding to an integrated luminosity of $4.4\,\text{fb}^{-1}$ at $\sqrt{s} = 13$ TeV. Events containing two well-reconstructed muons identified as such with $p_\text{T} > 400$ MeV are selected. Events with additional VELO tracks or photons, or with significant activity in HeRSCheL, are vetoed.

A two-dimensional fit to the dimuon mass and p_T^2 distributions is used to extract the exclusive J/ψ and $\psi(2S)$ yields in ten rapidity intervals. Three background sources are considered: Proton-dissociation events (PD), where either incoming proton does not survive the interaction; QED continuum dimuon production, where a pair of muons is exclusively produced via photon fusion; And feed-down from higher-mass charmonia, either $\psi(2S)$ or $\chi_{cJ}(1P)$ with $J = 0, 1, 2$, decaying to J/ψ.

Differential cross sections are calculated for J/ψ and $\psi(2S)$ production, as shown in Figure 1, and compared with theoretical predictions. The J/ψ cross section agrees with the NLO prediction [17], which improves over the LO prediction [18]. On the other hand, the $\psi(2S)$ cross section is significantly overestimated by both LO and NLO predictions [19].

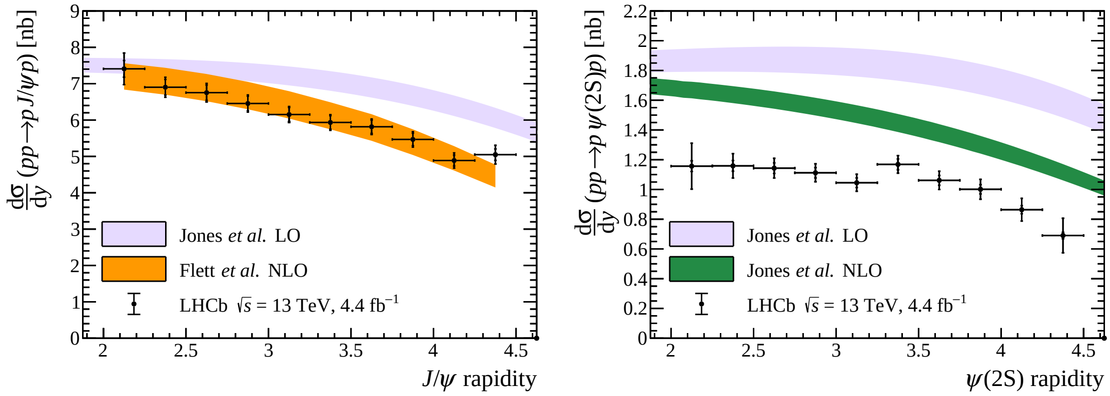

Figure 1: Differential cross-section for (left) J/ψ and (right) $\psi(2S)$ mesons. Theoretical predictions from Jones *et al.* [18, 19] and Flett *et al.* [17] are shown for comparison.

The J/ψ photoproduction cross-sections are calculated as a function of the photon-proton centre-of-mass energy, and the results are found to be consistent but more precise than those in the previous LHCb measurement [6]. Finally, the dependence of the J/ψ and $\psi(2S)$ cross sections on the total transverse momentum transfer is determined in pp collisions for the first time and is found to be consistent with the behavior observed at HERA [12].

4. Observation of exotic $J/\psi\phi$ resonant structure in diffractive processes in proton-proton collisions

The diffractive production of $J/\psi\phi$ vector mesons is studied [9] using data from proton-proton collisions corresponding to an integrated luminosity of 5 fb^{-1} at $\sqrt{s} = 13$ TeV. Several exotic states have previously been observed in the $J/\psi\phi$ mass spectrum in amplitude analyses of $B^+ \to J/\psi\phi K^+$ decays [20–22] at LHCb. Five of those exotic candidates, $\chi_{c1}(4140)$, $\chi_{c1}(4274)$ and $\chi_{c1}(4685)$ with quantum numbers $J^{PC} = 1^{++}$, and $\chi_{c0}(4500)$ and $\chi_{c0}(4700)$ with $J^{PC} = 0^{++}$, can be produced in photon-photon or pomeron-pomeron processes. Searches for the production of these exotic-hadron candidates in such processes can help elucidate their nature and distinguish between compact tetraquarks and molecular states [23–26].

Events containing two muons and two kaons identified as such with $p_{\mathrm{T}} > 200$ MeV are selected. Their invariant masses are required to satisfy $3036 < M_{\mu^+\mu^-} < 3156$ MeV, $1005 < M_{K^+K^-} < 1035$ MeV and $M_{J/\psi\phi} < 6000$ MeV, and events with additional VELO tracks are vetoed. A high-multiplicity control sample is constructed by inverting the offline requirement on the number of tracks, which is shown in Figure 2 (left). A fit is performed in this control sample with a model consisting of a sum of two exponential functions modified by a turn-on factor and convolved with a resolution function. Notably, no mass structure is visible when additional tracks are allowed. However, when the veto on additional tracks is imposed, a clear structure becomes visible in the $J/\psi\phi$ invariant mass distribution, which is shown in Figure 2 (right). A fit is performed on this distribution assuming the five states previously described and a non-resonant component, from which yields are extracted. The resonant states are described by relativistic Breit-Wigner functions, while the non-resonant component is described by a single exponential modified by the turn-on factor extracted from the control sample. All components are convolved with resolution functions.

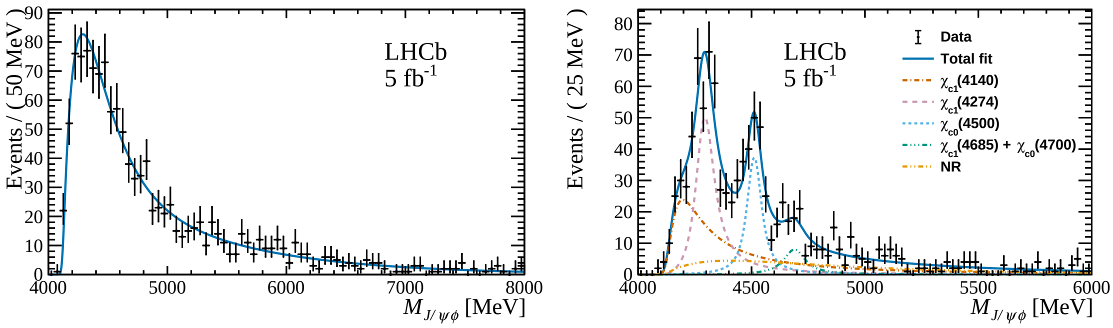

Figure 2: Invariant-mass distributions for $J/\psi(\to \mu^+\mu^-)\phi(\to K^+K^-)$ candidates (left) in the high-multiplicity control sample constructed by inverting the offline requirement on the number of tracks and (right) in the signal sample where the veto on additional reconstructed tracks is imposed. Fit results are overlaid on both distributions.

The $\chi_{c0}(4500)$ state is observed with a statistical significance above 6σ, while the $\chi_{c1}(4274)$ is confirmed with a significance larger than 4σ. Integrated cross-sections for each individual component, as well as the total $J/\psi(\to \mu^+\mu^-)\phi(\to K^+K^-)$ cross-section, are calculated in the fiducial region $2.0 < \eta(\mu^\pm, K^\pm) < 5.0$, $p_\mathrm{T}(\mu^\pm, K^\pm) > 200\,\mathrm{MeV}$, $M_{J/\psi\phi} < 6\,\mathrm{GeV}$ and reported as well. This is the first measurement of the $J/\psi(\to \mu^+\mu^-)\phi(\to K^+K^-)$ production cross section in events with no additional detected activity, where photon- and pomeron-induced processes are expected to dominate.

5. Study of exclusive photoproduction of charmonium in ultra-peripheral lead-lead collisions

The coherent production of J/ψ and $\psi(2S)$ vector mesons in ultra-peripheral PbPb collisions [8] is studied using data corresponding to an integrated luminosity of $228\,\mu\mathrm{b}^{-1}$ at $\sqrt{s} = 5.02\,\mathrm{TeV}$. Coherent UPC events are those where the photon couples coherently with the entire nucleus through the exchange of a pomeron, and the incoming nuclei are more likely to survive the interaction, unlike incoherent events, where the photon couples to individual nucleons and the incoming particles are more likely to break up. The coherent photoproduction of J/ψ and $\psi(2S)$ mesons in ultra-peripheral collisions is expected to probe the nuclear gluon PDF at a momentum transfer of about $M^2/4$, where M is the mass of the produced meson. This measurement may also help constrain theoretical predictions by restricting the choice of the meson wave function in dipole scattering models [27,28] and the factorization scale in perturbative QCD models [29].

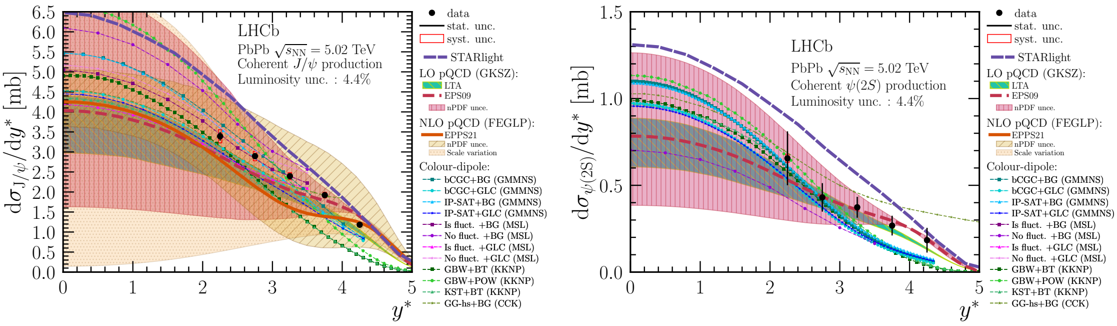

Figure 3: Differential cross-section as a function of the rapidity in the PbPb centre-of-mass reference frame (y^*) for coherent (left) J/ψ and (right) $\psi(2S)$ photoproduction, compared to theoretical predictions.

Differential cross-sections for coherent J/ψ and $\psi(2S)$ photoproduction, as a function of rapidity (y^*) and transverse momentum (p_T^*) in the PbPb centre-of-mass frame, are measured separately for the two mesons in the ranges $2.0 < y^* < 4.5$ and $0 < p_T^* < 0.2\,\text{GeV}/c$. The measurement as function of (y^*) is shown in Figure 3, and theoretical predictions are overlaid for comparison. The large uncertainties due to nuclear parton distribution functions (nPDF) indicate that coherent charmonium photoproduction in heavy ion collisions is very sensitive to the nuclear modification factors, especially to the modelling of the gluon shadowing, used in the LO pQCD calculations [29]. These are the most precise coherent J/ψ measurement to date and the first coherent $\psi(2S)$ measurement in the forward region. The ratio of the cross sections between the coherent $\psi(2S)$ and J/ψ production, as a function of y^*, is also determined for the first time in PbPb collisions and is found to be compatible with theoretical models.

6. Coherent photoproduction of ρ^0, ω and excited vector mesons in ultra-peripheral PbPb collisions

The coherent production of dipions in ultra-peripheral PbPb collisions [13] is studied using data corresponding to an integrated luminosity of $224.6\,\mu\text{b}^{-1}$ at $\sqrt{s} = 5.02$ TeV. This final state is dominated by the ρ^0 meson, but contributions from the ω and other excited states also need to be taken into account. At LHCb, the coherent photoproduction of ρ^0 mesons in ultra-peripheral PbPb collisions can probe the nuclear gluon PDF at Bjorken-x values down to 10^-6, and therefore may help understand nuclear shadowing effects at low-x.

Events containing two pions within the range $2 < \eta < 5$ with $p_T > 100$ MeV and $M_{\pi\pi} > 400$ MeV are selected. To select coherent events, it is required that no additional tracks were reconstructed and that the activity in HeRSCheL is consistent with noise. The resulting dipion invariant mass spectrum is fitted with several models of increased complexity. Achieving a consistent description across the full invariant-mass range requires including contributions from the ρ^0, ω, two additional excited states and a nonresonant contribution. The two excited states are found to be compatible with the $\rho(1450)$ and the $\rho(1700)$.

The differential cross-sections for coherent photoproduction of ρ^0, ω and the excited states are measured as functions of rapidity. The ρ^0 measurements are shown in Fig. 4 and compared with theoretical predictions. In Fig. 4 (left), the GKZ model [30] is overlaid, which includes

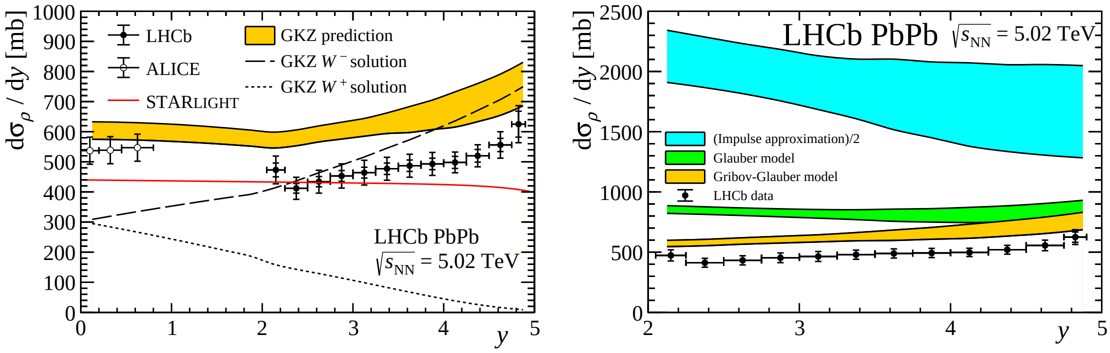

Figure 4: Differential cross-section for coherent ρ^0 photoproduction as a function of rapidity. The LHCb error bars represent the statistical and total uncertainties. (left) The GKZ prediction is shown. The contributions due to the photon emitted from each ion, W^+ and W^-, are explained in Ref. [13]. Also shown are ALICE results at central rapidity and the output of the STARLIGHT generator. (right) Predictions from the impulse approximation, Glauber model, and Gribov–Glauber model are shown.

linear and nonlinear QCD effects using a Gribov–Glauber calculation to describe multiple nucleon interactions. It correctly reproduces the slow rise with rapidity seen in data, but it overestimates the observed cross-sections by about 30%, indicating that additional suppression is required. In Fig. 4 (right), the measurement is compared against predictions from an Impulse Approximation model (no shadowing) [31], a Glauber model calculation (shadowing from elastic scatters only) and a Gribov–Glauber calculation (with both elastic and inelastic scatters) [32]. Best agreement is achieved by the Gribov-Glauber model, showing that elastic and inelastic rescattering effects have a major impact on the result, but again additional suppression is needed. The coherent ω cross-section is found to be about a factor ten lower than that of the ρ^0 meson, in agreement with photoproduction measurements performed at HERA.

7. First observation of the $\phi(1020)$ meson in the K^+K^- mass spectrum of ultra-peripheral PbPb collisions at forward rapidity

The production of kaon pairs in ultra-peripheral PbPb interactions [10] is studied using data corresponding to an integrated luminosity of 228 μb^{-1} at $\sqrt{s} = 5.02$ TeV. Events containing exactly two reconstructed kaons and no activity above noise in HeRSCheL are selected. The $\phi(1020)$ decay vertex position is required to be compatible with the collision region to suppress background from electron pairs coming from converted photons. The resulting invariant-mass spectrum reveals multiple peaking structures, including contributions from misidentified $\rho^0(770) \to \pi^+\pi^-$ and $J/\psi \to p\overline{p}$ decays, as illustrated in Figure 5 (left). A fit is performed on the low invariant-mass region $M_{K^+K^-} < 1450$ MeV, taking into account contributions from exclusive $\phi(1020) \to K^+K^-$, nonresonant K^+K^- production, dissociative production (where either nucleus does not survive the interaction) and misidentified $\rho^0(770) \to \pi^+\pi^-$ decays. The fit results are shown in Figure 5, and the $\phi(1020)$ peak is observed with a significance that exceeds 5σ. This is the first observation of the $\phi(1020)$ meson in the invariant-mass spectrum of K^+K^- meson pairs produced in ultra-peripheral PbPb interactions at forward rapidity.

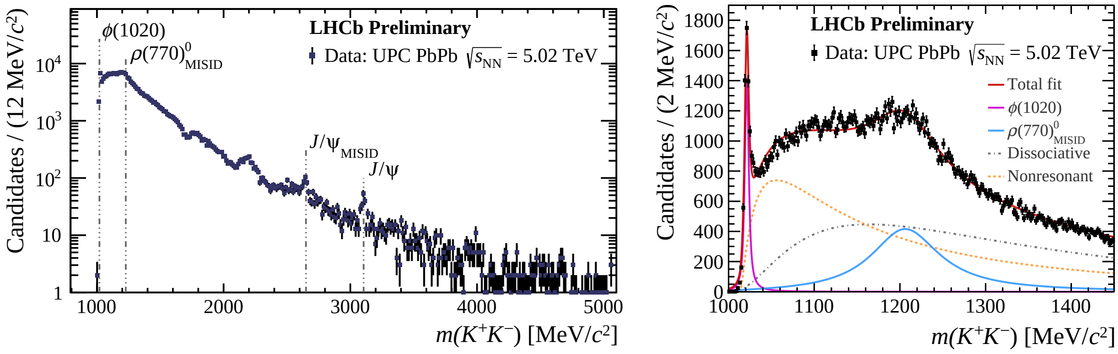

Figure 5: Invariant-mass distribution of dikaons in elastic-enriched ultra-peripheral PbPb collisions. (left) Contributions associated with $\phi(1020)$ and J/ψ as well as misidentified $\rho^0(770) \to \pi^+\pi^-$ and $J/\psi \to p\overline{p}$ decays are seen. (right) The low-mass region is show with fit results overlaid. The ϕ resonance is clear, followed by the wider peak attributed to misidentified $\rho^0(770) \to \pi^+\pi^-$ decays.

8. Photon triggers for ultra-peripheral lead-lead collisions in Run 2 and Run 3

Studies of photon-photon scattering in PbPb collisions have been largely discussed in recent years due to the possibility to search for undiscovered phenomena [33]. It has been shown that LHCb is sensitive to UPC production of hypothetical axion-like particles [34] and low-mass resonances [35]. The study of UPC events with photons in the final state requires triggering on low-multiplicity events with at least one reconstructed photon [36]. This is challenging since photons are copiously produced in PbPb collisions and the purity of simplified photon reconstruction is usually low, specially at low transverse energy, E_{T}.

Figure 6 compares the E_{T} distributions of photon pair candidates produced in PbPb collisions using Run 2 (2018) and Run 3 (2023) data at $\sqrt{s}$ = 5.02 and 5.36 TeV, respectively. Both samples correspond to an integrated luminosity of about 0.2 nb^{-1}. In 2018, the photon pairs are selected with a hardware trigger while for 2023 data set, they are selected with a fully-software trigger. Due to the E_{T} threshold applied in 2018, there are no diphoton candidates with leading photon E_{T} below 1000 MeV while for 2023 data set the trigger threshold was moved to 200 MeV. Therefore, low-mass resonances studies can be performed with the Run 3 data set.

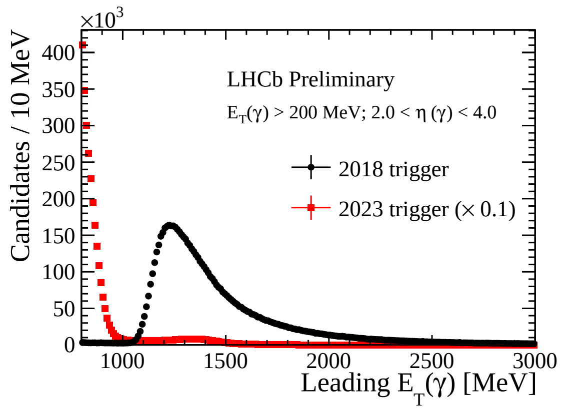

Figure 6: Leading photon E_{T} from photon pairs in data taken in 2018 (Run 2) and 2023 (Run 3).

References

[1] C. A. Bertulani, S. R. Klein, and J. Nystrand, *Physics of ultra-peripheral nuclear collisions*, Ann. Rev. Nucl. Part. Sci. **55** (2005) 271, `arXiv:nucl-ex/0502005`.

[2] LHCb collaboration, R. Aaij *et al.*, *Exclusive J/ψ and $\psi(2S)$ production in pp collisions at $\sqrt{s}$ =7 TeV*, J. Phys. **G40** (2013) 045001, `arXiv:1301.7084`.

[3] LHCb collaboration, R. Aaij *et al.*, *Updated measurements of exclusive J/ψ and $\psi(2S)$ production cross-sections in pp collisions at $\sqrt{s}$ =7 TeV*, J. Phys. **G41** (2014) 055002, `arXiv:1401.3288`.

[4] LHCb collaboration, R. Aaij *et al.*, *Observation of charmonium pairs produced exclusively in pp collisions*, J. Phys. **G41** (2014) 115002, `arXiv:1407.5973`.

[5] LHCb collaboration, R. Aaij *et al.*, *Measurement of the exclusive $\Upsilon(nS)$ production cross-section in pp collisions at $\sqrt{s}$ =7 TeV and 8 TeV*, JHEP **09** (2015) 084, `arXiv:1505.08139`.

[6] LHCb collaboration, R. Aaij *et al.*, *Central exclusive production of J/ψ and $\psi(2S)$ mesons in pp collisions at $\sqrt{s}$ =13 TeV*, JHEP **10** (2018) 167, `arXiv:1806.04079`.

[7] LHCb collaboration, R. Aaij *et al.*, *J/ψ photo-production in Pb-Pb peripheral collisions at $\sqrt{s_{NN}} = 5$ TeV*, Phys. Rev. **C105** (2020) L032201, `arXiv:2108.02681`.

[8] LHCb collaboration, R. Aaij *et al.*, *Study of exclusive photoproduction of charmonium in ultra-peripheral lead-lead collisions*, JHEP **06** (2023) 146, `arXiv:2206.08221`.

[9] LHCb collaboration, R. Aaij *et al.*, *Observation of exotic $J/\psi\phi$ resonant structure in diffractive processes in proton-proton collisions*, Phys. Rev. Lett. **134** (2025) 031902, `arXiv:2407.14301`.

[10] LHCb collaboration, *First observation of the $\phi(1020)$ meson in the K^+K^- mass spectrum of ultra-peripheral PbPb collisions at forward rapidity*, LHCb-CONF-2024-006, 2024.

[11] LHCb collaboration, R. Aaij *et al.*, *Study of charmonium production via the decay to $p\bar{p}$ at $\sqrt{s} = 13$ TeV*, Eur. Phys. J. **C84** (2024) 1274, `arXiv:2407.14261`.

[12] LHCb collaboration, R. Aaij *et al.*, *Measurement of exclusive J/ψ and $\psi(2S)$ production at $\sqrt{s} = 13$ TeV*, SciPost Phys. **18** (2025) 071, `arXiv:2409.03496`.

[13] LHCb collaboration, R. Aaij *et al.*, *Coherent photoproduction of ρ^0, ω and excited vector mesons in ultraperipheral PbPb collisions*, `arXiv:2506.06250`, Submitted to JHEP.

[14] LHCb collaboration, A. A. Alves Jr. *et al.*, *The LHCb detector at the LHC*, JINST **3** (2008) S08005.

[15] LHCb collaboration, R. Aaij *et al.*, *LHCb detector performance*, Int. J. Mod. Phys. **A30** (2015) 1530022, `arXiv:1412.6352`.

[16] K. Carvalho Akiba *et al.*, *The HeRSCheL detector: high-rapidity shower counters for LHCb*, JINST **13** (2018) P04017, arXiv:1801.04281.

[17] C. A. Flett, A. D. Martin, M. G. Ryskin, and T. Teubner, *Very low x gluon density determined by LHCb exclusive J/ψ data*, Phys. Rev. **D102** (2020) 114021, arXiv:2006.13857.

[18] S. P. Jones, A. D. Martin, M. G. Ryskin, and T. Teubner, *Probes of the small x gluon via exclusive J/ψ and Υ production at HERA and the LHC*, JHEP **11** (2013) 085, arXiv:1307.7099.

[19] S. P. Jones, A. D. Martin, M. G. Ryskin, and T. Teubner, *Predictions of exclusive $\psi(2S)$ production at the LHC*, J. Phys. **G41** (2014) 055009, arXiv:1312.6795.

[20] LHCb collaboration, R. Aaij *et al.*, *Observation of exotic $J/\psi\phi$ structures from amplitude analysis of $B^+ \to J/\psi\phi K^+$ decays*, Phys. Rev. Lett. **118** (2017) 022003, arXiv:1606.07895.

[21] LHCb collaboration, R. Aaij *et al.*, *Amplitude analysis of $B^+ \to J/\psi\phi K^+$ decays*, Phys. Rev. **D95** (2017) 012002, arXiv:1606.07898.

[22] LHCb collaboration, R. Aaij *et al.*, *Observation of new resonances decaying to $J/\psi K^+$ and $J/\psi\phi$* , Phys. Rev. Lett. **127** (2021) 082001, arXiv:2103.01803.

[23] S. J. Brodsky and R. F. Lebed, *QCD dynamics of tetraquark production*, Phys. Rev. **D91** (2015) 114025.

[24] A. Cerri *et al.*, *Opportunities in flavour physics at the HL-LHC and HE-LHC*, CERN Yellow Rep. Monogr. **7** (2019) 867, arXiv:1812.07638.

[25] A. Esposito, C. A. Manzari, A. Pilloni, and A. D. Polosa, *Hunting for tetraquarks in ultraperipheral heavy ion collisions*, Phys. Rev. **D104** (2021) 114029.

[26] A. Esposito, F. Piccinini, A. Pilloni, and A. D. Polosa, *A mechanism for hadron molecule production in $p\overline{p}(p)$ collisions*, Journal of Modern Physics **4** (2013) 1569.

[27] H. Kowalski, L. Motyka, and G. Watt, *Exclusive diffractive processes at HERA within the dipole picture*, Phys. Rev. **D74** (2006) 074016, arXiv:hep-ph/0606272.

[28] V. P. Gonçalves and M. V. T. Machado, *Vector meson production in coherent hadronic interactions: an update on predictions for RHIC and LHC*, Phys. Rev. **C84** (2011) 011902, arXiv:1106.3036.

[29] V. Guzey, E. Kryshen, and M. Zhalov, *Coherent photoproduction of vector mesons in ultra-peripheral heavy ion collisions: Update for run2 at the CERN Large Hadron Collider*, Phys. Rev. **C93** (2016) 055206, arXiv:1602.01456.

[30] V. Guzey, E. Kryshen, and M. Zhalov, *Coherent photoproduction of vector mesons in ultraperipheral heavy ion collisions: Update for run 2 at the cern large hadron collider*, Phys. Rev. C **93** (2016) 055206.

[31] G. F. Chew and G. C. Wick, *The impulse approximation*, Phys. Rev. **85** (1952) 636.

[32] L. Frankfurt, V. Guzey, M. Strikman, and M. Zhalov, *Nuclear shadowing in photoproduction of ρ mesons in ultraperipheral nucleus collisions at rhic and the lhc*, Physics Letters B **752** (2016) 51.

[33] S. R. Klein and P. Steinberg, *Photonuclear and two-photon interactions at high-energy nuclear colliders*, Annual Review of Nuclear and Particle Science **70** (2020) 323.

[34] V. P. Gonçalves, D. E. Martins, and M. S. Rangel, *Searching for axionlike particles with low masses in ppb and pbpb collisions*, The European Physical Journal C **81** (2021) 522.

[35] M. Kłusek-Gawenda, R. McNulty, R. Schicker, and A. Szczurek, *Light-by-light scattering in ultraperipheral heavy-ion collisions at low diphoton masses*, Phys. Rev. D **99** (2019) 093013.

[36] LHCb collaboration, *Photon triggers for ultra-peripheral lead-lead collisions in Run 2 and Run 3*, LHCB-FIGURE-2024-012, 2024.